energies

MDPI

Article

A Design of a 2-DoF Planar Parallel Manipulator with an Electro-Pneumatic Servo-Drive

Jakub Takosoglu *, Urszula Janus-Galkiewicz and Jarosław Galkiewicz

Faculty of Mechatronics and Mechanical Engineering, Kielce University of Technology, Aleja Tysiaclecia Panstwa Polskiego 7, 25-314 Kielce, Poland
* Correspondence: qba@tu.kielce.pl

Abstract: This paper presents the design of a planar parallel manipulator with a pneumatic drive. Such manipulators are used in production lines for sorting, selecting, packing, and palletizing workpieces. This paper presents simulation studies of the designed manipulator in Matlab/Simulink software and using the SimMechanics library. A simple kinematics problem and an inverse kinematics problem were solved in order to carry out simulation studies of the designed manipulator. Simulation studies were also carried out on the dynamics of the manipulator using a mathematical model describing the physical phenomena occurring during the operation of the manipulator's electro-pneumatic servo-drives. The main objective of the simulation study was to determine the manipulator working space and the possibility of positional control of the manipulator end-effector using a fuzzy logic controller.

Keywords: planar parallel manipulator; fuzzy logic controller; pneumatic positioning system; electro-pneumatic servo-drive

Citation: Takosoglu, J.; Janus-Galkiewicz, U.; Galkiewicz, J. A Design of a 2-DoF Planar Parallel Manipulator with an Electro-Pneumatic Servo-Drive. *Energies* **2022**, *15*, 8482. https://doi.org/10.3390/en15228482

Academic Editors: Mohsin Jamil, Krzysztof Szabat and Marcin Kaminski

Received: 5 July 2022
Accepted: 9 November 2022
Published: 13 November 2022

Publisher's Note: MDPI stays neutral with regard to jurisdictional claims in published maps and institutional affiliations.

1. Introduction

The majority of pneumatically driven industrial robots and manipulators in use today are applied in sorting, selection, packaging, palletizing, assembly, or other industrial applications requiring only a few main (resulting from the actuator stroke) positions. The most commonly used are standard pneumatic actuators, which provide high dynamics of operation, overload capacity, accuracy, and repeatability. However, these uses do not allow the actuator piston to be placed in all possible positions that could be desired. This is a direct result of the properties of the standard pneumatic drive (which can only assume the two extreme piston positions) and the working medium, which is compressed air. Complex friction processes [1] occurring in pneumatic actuators and the stick–slip phenomenon [2] also adversely affect the process of positioning and achieving precise movements of the actuator piston. Pneumatic robots and manipulators use electro-pneumatic servos for positional control. They are most commonly constructed with the use of rodless actuators with an integrated internal piston position sensor, a flow or pressure proportional valve, and a negative feedback control system.

Pneumatic manipulators are mainly designed as systems with serial kinematics. A decisive factor influencing the positioning accuracy of manipulators is the rigidity of the structure. The series-built drive axes deform elastically under the influence of the masses of the conveyed objects and the drives themselves, which leads to the summation of deformations at the end of the kinematic chain and a deterioration in positioning accuracy. A number of simulation and experimental studies have been conducted on multi-axis serial pneumatic manipulators [3,4]. Based on the analysis of the test results, it was found that the positioning accuracy of the manipulator end-effector is several times lower than for a single pneumatic drive axis. The kinematic structure that allows for the reduction in positioning errors due to the peculiarities of serial manipulators is based on closed kinematic chains of so-called parallel structures. Manipulators with parallel structures

have kinematic pairs connected in parallel, forming a closed kinematic chain [5,6]. Such manipulators are characterized by high stiffness, low inertia, high load capacity, and high positioning accuracy compared with serial manipulators [7–13]. Parallel manipulators and hybrid manipulators are currently the areas of mechatronics that are developing the most [14,15]. The disadvantages of robots and manipulators with parallel structure are a smaller working space, and a more complex control system.

In this article, the control system is based on the fuzzy logic controller. Fuzzy logic controllers are recently more and more popular in pneumatic systems [16]. There are different approaches to applications of fuzzy logic controllers [5,17]. Different methods can support controllers to obtain a better quality of control [18]. Manipulators and parallel robots are used in industry for palletizing, sorting, or assembling parts, as well as in medical technology for rehabilitation, laparoscopy, or endoscopy.

The structure of this article is as follows: first, a 3D model of the manipulator is presented, then, the kinematics, working space, and dynamics of the manipulator are described. The paper ends with simulation studies. The details of the parallel manipulator control system using a PD-type fuzzy logic controller, and the results of the experimental studies on the prototype are presented in the second part.

2. Solid Model of the Manipulator

The solid model of the manipulator was designed in a 3D space using SolidWorks software. Figure 1 presents a proposed model of a planar manipulator with two degrees of freedom with a linear drive. The manipulator consists of two rodless actuators with an integrated internal measurement of the position and speed of the piston of the actuator, two rigid arms made of aluminium profiles, four bearings connecting the actuators to the arms, the end-effector, and the base, to which the manipulator is attached. The actuators are attached to the base in such a way that their carriages point inwards. Mounting plates with bearings are attached to the carriages. The manipulator's arms are placed between the bearings, which limits the movement to only one plane. At the opposite ends of the arms, bushings are set in holes and connected by a pin to which the manipulator end-effector was attached.

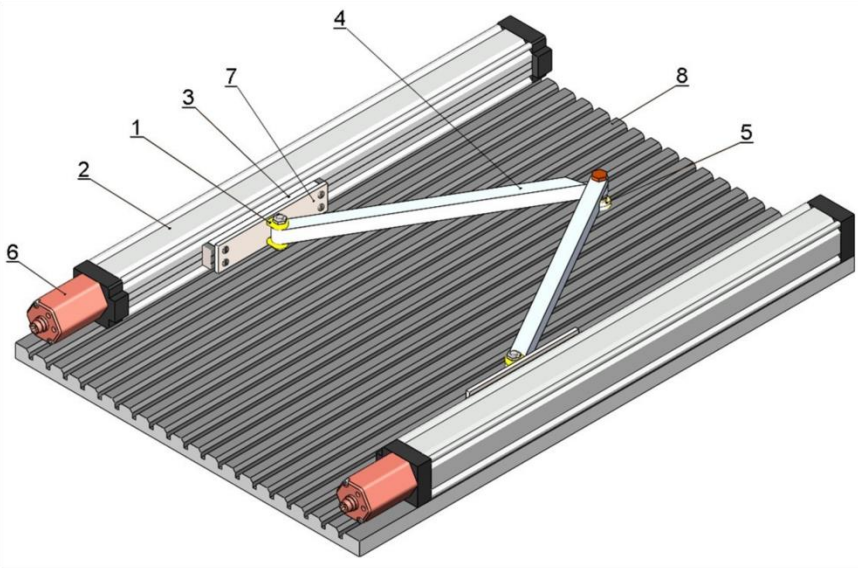

Figure 1. A solid model of a parallel manipulator (1—bearing, 2—actuator, 3—actuators, 4—arm, 5—end-effector, 6—position transducer, 7—mounting plates, 8—base).

The arms of the designed manipulator are connected by rotary joints to prismatic-type drives. The drives are placed parallel to each other, defining the working plane. Each arm has only class V kinematic pair connections in the kinematic chain (only one degree of

freedom in the relative motion of its links and five imposed connection conditions). The ends of the arms are connected by joints with a common axis of rotation, forming a working platform for fixing the manipulator end-effector.

Figure 2 shows the four extreme end-effector positions obtained for maximum actuator extensions.

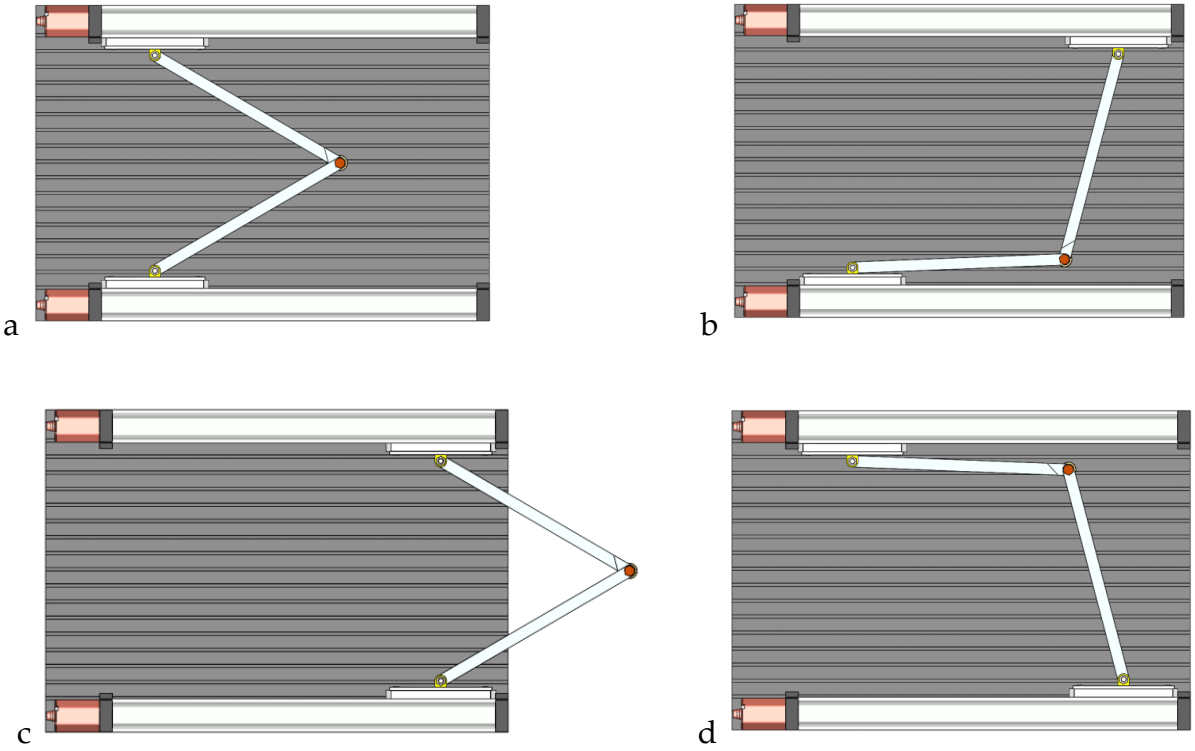

Figure 2. Extreme positions of the manipulator end-effector: both sliders at the minimum position (**a**), left slider at the maximum position and right slider at the minimum position (**b**), both sliders at the maximum position (**c**), left slider at the minimum position and right slider at the maximum position (**d**).

During design, the length of the arms was assumed to be greater than half the width of the working surface. The advantage of such a solution is an unambiguous control method, since the extension of the actuator carriages determines only one possibility of positioning the end-effector. Manipulators of this type more often operate in a vertical orientation than a horizontal one. However, the designed manipulator was oriented horizontally in order to more effectively illustrate the positioning capabilities of the end-effector. In industrial conditions, it is recommended to orient the manipulator in such a position that the technological forces applied to the end-effector work along the axis of the arms and the drives themselves, i.e., to only cause them to apply tension or compress. The action of tensile and compressive forces is a consequence of the articulated connection of the projected manipulator arms, and the condition of machines with closed kinematic chains.

3. Kinematics of the Manipulator

The manipulator hinges are described using the internal coordinate q_i where $i = 1, 2, 3, \ldots, N$ denotes the degrees of freedom of the nodes. Variables q_i, when combined, form vector $q = (q_1, q_2, q_3, \ldots, N)^T \in Q$ called the internal coordinate vector. In the designed case the manipulator is a control system, therefore q corresponds to a state vector. When designing a manipulator, it is necessary to determine the position and orientation of its end-effector as defined in external coordinates, using vector $(x, y, z, \alpha, \beta, \gamma)^T \in R^6$, and as a function of internal coordinates $(q_1, q_2, q_3, \ldots, N)^T \in Q$. The transformation

$Q \rightarrow R^6$ represents the manipulator kinematics in coordinates. The study includes changes in the position, velocity, and acceleration of each manipulator component, and, in particular, of the end-effector without taking into account the forces producing the motion. To solve the simple and inverse kinematics problem, a computational diagram of the manipulator kinematics was constructed with the variables plotted, as shown in Figure 3.

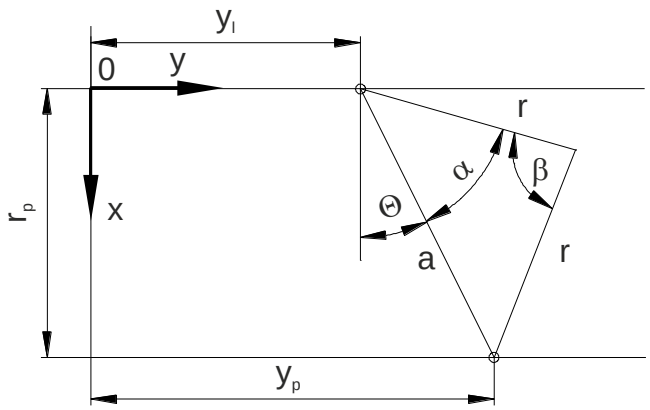

Figure 3. Calculation scheme of manipulator kinematics.

The following variable designations were adopted:

r_p—actuator spacing;

r—arm length;

a—distance between the carriage of the first actuator and the carriage of the second actuator;

y_1—distance of the carriage of the first actuator from the initial position;

y_2—distance of the second actuator carriage from the initial position;

α—angle between the length of the arm and the distance between the actuator carriages;

β—angle between the robot's arms;

θ—angle between the spacing of the actuators and the distance between the actuator carriages.

4. Simple Kinematics

Simple kinematics involves calculating the position and orientation of the end-effector from the data on articulated variables. Knowing the configuration coordinates, the position of a given point associated with the manipulator relative to the global coordinate system is calculated, i.e., it is a description of the manipulator position in configuration coordinate space into a description in Cartesian coordinate space. The relationships resulting from the isosceles triangle shown in Figure 3 were used to determine the position of the end-effector of the designed manipulator:

$$a = \sqrt{r_p^2 + (y_p - y_l)} \tag{1}$$

$$\beta = \arccos\left(1 - \frac{a^2}{2r^2}\right) \tag{2}$$

From the determined dependences (1) and (2), the following was obtained:

$$2 \cdot r > a \tag{3}$$

and therefore:

$$\alpha = \frac{\pi - \beta}{2} \tag{4}$$

$$\theta = \arctan\left(\frac{y_p - y_l}{r_p}\right) \tag{5}$$

The position of the manipulator end-effector is determined by variables x and y:

$$x = r \cdot \cos(\alpha + \beta) \tag{6}$$

$$y = y_l + r \cdot \sin(\alpha + \beta) \tag{7}$$

5. Working Space

The working space is limited by the geometry of the manipulator, and the mechanical constraints. The extent of the end-effector's working movement is naturally limited by the spacing of the guides and their length. The lateral edges of the working space are straight lines whose length is equal to the difference in length of the guides l_p and the length of the arm r. The upper edge is made up of two curves l_3 and l_4, and the lower edge is made up of curves l_1 and l_2. The working space is shown in Figure 4, with the symbols plotted.

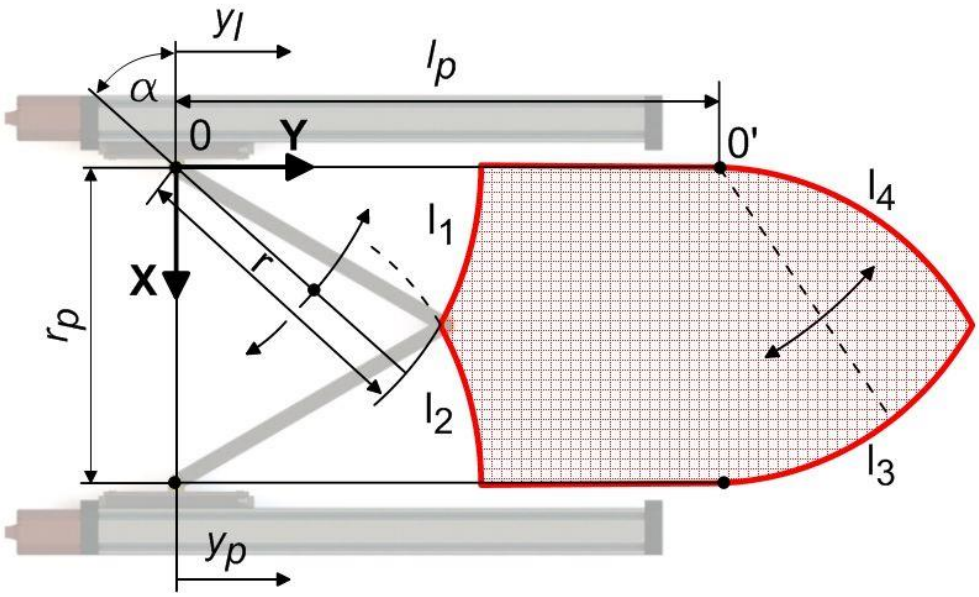

Figure 4. Manipulator working space.

The equation describing curves $l_1(l_2)$ is obtained by setting the left (right) actuator slider to the extreme lower position $y_l = 0$ ($y_p = 0$) and moving the right (left) actuator slider from the extreme lower position upwards (increasing the y_p-coordinate) until $y_p = r$. The movement of the end-effector along line l_1 is then described by the equations:

$$x_e = r \cdot \cos(\alpha) \tag{8}$$

$$y_e = r \cdot \sin(\alpha) \tag{9}$$

where: α—angle between the left arm and the 0X-axis (Figure 3).

Analogous equations are derived for the remaining edges. In the case of edges l_3 and l_4, the left carriage was placed in the extreme upper position ($y_l = l_p$), whereas the right actuator carriage, after being placed at the same height, was moved by a distance corresponding to the length of the arm to the position $y_p = l_p - r$.

6. Dynamics of the Manipulator

The study of the dynamics of the planar-parallel manipulator was carried out on the mathematical model of the electro-pneumatic servo-drive developed by Takosoglu J. [19]. The above-mentioned paper presents a complete derivation of the differential equations describing the dynamics and detailed computational models of the electro-pneumatic servo-drive, flow control servo-valve, friction forces, electromagnetic transducer, and servo-valve

distributor. The nonlinear dynamic model of an electro-pneumatic servo-drive controlled by a flow control servo-valve is described by the following differential equations:

- Equation of motion for the piston—slide of the rodless actuator:

$$\frac{d^2y}{dt^2} = \frac{1}{M+m}\left\{A\Delta p - \left[f_l v + F_k \mathrm{sgn}(v) + F_{pr} e^{\left(-\frac{v}{v_k}\right)} \mathrm{sgn}(v) + k_p|\Delta p|\right] + m\ g\ \sin\alpha\right\} \quad (10)$$

where:

y, v—displacement and velocity of the piston—slide;
A—area of piston;
Δp—pressure difference between cylinder chambers; $\Delta p = p_1 - p_2$
p_1, p_2—absolute pressures in cylinder's chambers;
M—mass of piston and slide;
f_l—viscous friction coefficient;
F_k—kinetic friction force (Coulomb friction force);
v_k—critical value of velocity, characteristic velocity of the Stribeck friction;
F_{pr}—break away force;
k_p—friction coefficient dependent upon seal dimensions;
m—initial load mass;
g—acceleration of gravity;
α—servo-motor infliction angle.

- Equation of motion for the spool of proportional directional control valve:

$$\frac{d^2x_r}{dt^2} = \frac{1}{m_r}\left\{\frac{k_m}{R_c}(u - nBl_c v_r)\left(1 - e^{\frac{R_c}{L}t}\right) - f_t v_r - k_s x_r\right\} \quad (11)$$

where:

x_r, v_r—displacement and velocity of valve spool;
m_r—mass of spool;
k_m—coefficient of electromechanical force transducer;
R_c—resistance of the solenoid;
u—coil voltage;
n—number of coils;
B—magnetic induction;
l_c—length of coil;
L—inductance of the solenoid;
f_t—coefficient of viscous friction;
k_s—spool spring rate.

- Equations for pressure in cylinder chambers:

$$\begin{array}{l} \frac{dp_1}{dt} = \frac{\kappa}{A(l_0+y)}\left\{R\frac{dm_1}{dt} - p_1 A v - \frac{\kappa-1}{\kappa}\alpha[A_{10}(T_1 - T_a) + A(T_1 - T_2)]\right\} \\ \frac{dp_2}{dt} = \frac{\kappa}{A\ (l+l_0-y)}\left\{-R\frac{dm_2}{dt} + p_2 A v - \frac{\kappa-1}{\kappa}\alpha[A_{20}(T_2 - T_a) + A(T_2 - T_1)]\right\} \end{array} \quad (12)$$

where:

κ—adiabatic exponent;
l_0—length of dead zone of the pneumatic cylinder;
l—stroke length of pneumatic cylinder;
R—specific gas constant;
α—overall heat-transfer coefficient;
T_1, T_2—temperature in cylinder chambers;
T_a—ambient temperature;
A_{10}, A_{20}—heat transfer surface;
$\frac{dm_1}{dt}$, $\frac{dm_2}{dt}$—mass flow rate.

- Equations for temperature in cylinder chamber:

$$\frac{dT_1}{dt} = \frac{\kappa T_1}{p_1 A_{01}(l_0+y)}\left\{R\left[\left(T_z - \frac{T_1}{\kappa}\right)\frac{dm_{14}}{dt} - \frac{\kappa-1}{\kappa}T_1\frac{dm_{45}}{dt}\right] - \frac{\kappa-1}{\kappa}\left[p_1 A_{01}\frac{dy}{dt} + \alpha_Q[A_1(T_1 - T_a) + A_{01}(T_1 - T_2)]\right]\right\} \quad (13)$$

$$\frac{dT_2}{dt} = \frac{\kappa T_2}{p_2 A_{02}(l_0+l-y)}\left\{R\left[\left(T_z - \frac{T_2}{\kappa}\right)\frac{dm_{12}}{dt} - \frac{\kappa-1}{\kappa}T_2\frac{dm_{23}}{dt}\right] + \frac{\kappa-1}{\kappa}\left[p_2 A_{02}\frac{dy}{dt} + \alpha_Q[A_2(T_2 - T_a) + A_{02}(T_2 - T_1)]\right]\right\} \quad (14)$$

- Equations for mass flow rate through proportional control valve:

$$\begin{aligned}\frac{dm_1}{dt} &= C_{14}\rho_0\sqrt{\frac{T_0}{T_z}}p_z w_{14} - C_{45}\rho_0\sqrt{\frac{T_0}{T_1}}p_1 w_{45}\\ \frac{dm_2}{dt} &= C_{23}\rho_0\sqrt{\frac{T_0}{T_2}}p_2 w_{23} - C_{12}\rho_0\sqrt{\frac{T_0}{T_z}}p_z w_{12}\end{aligned} \quad (15)$$

where:

ρ_0—air density in the normal reference atmosphere (ANR);

T_0—normal ambient temperature;

p_z—air supply pressure;

T_z—air supply temperature;

C_{14}, C_{45}, C_{12}, C_{23}—sonic conductance consistent with the standard ISO 6358-1989 for critical pressure ratio.

$$\begin{cases} C_{14} \approx \alpha_{14}\frac{A_{14}\psi_{\max}}{p_0}\sqrt{2R_0T_0} \\ C_{45} \approx \alpha_{45}\frac{A_{45}\psi_{\max}}{p_0}\sqrt{2R_0T_0} \\ C_{12} \approx \alpha_{12}\frac{A_{12}\psi_{\max}}{p_0}\sqrt{2R_0T_0} \\ C_{23} \approx \alpha_{23}\frac{A_{23}\psi_{\max}}{p_0}\sqrt{2R_0T_0} \end{cases} \quad (16)$$

where:

α_{14}, α_{45}, α_{12}, α_{23}—flow resistance coefficients considered in real flows;

ψ_{14}, ψ_{45}, ψ_{12}, ψ_{23}—distributor's flow functions on routes 1→4, 4→5, 1→2, 2→3, reaching maximum ψ_{max} = 0.4842 for critical pressure ratio b = 0.528;

w_{14}, w_{45}, w_{12}, w_{23}—nonlinear flow function (sonic flow and subsonic flow) depending on the pressure ratio and on the critical pressure ratio.

$$w_{14} = \begin{cases} 1 & 0 \le \frac{p_1}{p_z} \le b_{12} \\ \sqrt{1 - \left(\frac{\frac{p_1}{p_z} - b_{14}}{1 - b_{14}}\right)^2} & b_{12} \le \frac{p_1}{p_z} \le 1, \end{cases}$$

and

$$w_{45} = \begin{cases} 1 & 0 \le \frac{p_a}{p_2} \le b_{45} \\ \sqrt{1 - \left(\frac{\frac{p_a}{p_2} - b_{45}}{1 - b_{45}}\right)^2} & b_{45} \le \frac{p_a}{p_2} \le 1, \end{cases}$$

and

$$w_{12} = \begin{cases} 1 & 0 \le \frac{p_1}{p_z} \le b_{12} \\ \sqrt{1 - \left(\frac{\frac{p_1}{p_z} - b_{12}}{1 - b_{12}}\right)^2} & b_{12} \le \frac{p_1}{p_z} \le 1, \end{cases} \quad (17)$$

and

$$w_{23} = \begin{cases} 1 & 0 \le \frac{p_a}{p_2} \le b_{23} \\ \sqrt{1 - \left(\frac{\frac{p_a}{p_2} - b_{23}}{1 - b_{23}}\right)^2} & b_{23} \le \frac{p_a}{p_2} \le 1 \end{cases}$$

where:

b_{14}, b_{45}, b_{12}, b_{23}—critical pressure ratio (a constant value b = 0.28 was assumed in the simulation model).

7. Simulation Studies

Based on the kinematic model of the manipulator and the dynamic electro-pneumatic servo-drive, a simulation study of the positioning of the parallel end-effector of a planar manipulator with electro-pneumatic drive using a fuzzy logic controller was carried out. A PD-type fuzzy logic controller developed by the authors was used, which is described in detail in papers [2,6].

Fuzzy logic systems are considered expert systems. The main element of the system is the knowledge base containing a set of rules which, when combined with the fuzzy sets theory, create the control algorithm. The algorithm joins human experience and intuition with an understanding of the behavior of the plant under control. The main advantage of fuzzy logic systems is the abandonment of an analytical description [20].

The control system is based on a set of IF-THEN conditions [20] as in (18):

$$u(k) = F[e(k), e(k-1), \ldots, e(k-v), u(k-1), u(k-2), \ldots, u(k-v)] \tag{18}$$

where the non-linear function F represents the rules of the controller. Function F describes the dependence of the error $e(k)$ and its change $\Delta e(k)$ on the control signal $u(k)$.

Variables of the process status, of the control, of the content of the antecedent, and the consequent of each rule determine the type of controller. The state variables utilized in the IF part can be taken as follows:

- Control error e;
- Control error change Δe;
- Control error sum δe;
- The control variables used in the THEN part can be taken as follows;
- Control signal u;
- Control signal change Δu.

Listed quantities are computed in the standard way, that is,

$$\begin{aligned} e(k) &= y_0(k) - y(k) \\ \Delta e(k) &= e(k) - e(k-1) \\ \Delta(\Delta e(k)) &= e(k) - 2e(k-1) + e(k-2) \\ \delta e(k) &= \sum_{i=1}^{k} e(i) \\ \Delta u(k) &= u(k) - u(k-1) \end{aligned} \tag{19}$$

where:

$y_0(k)$—set-point (input function);

$y(k)$—output of the plant (response).

PID fuzzy logic controllers can be implemented in direct or incremental versions (Figure 5).

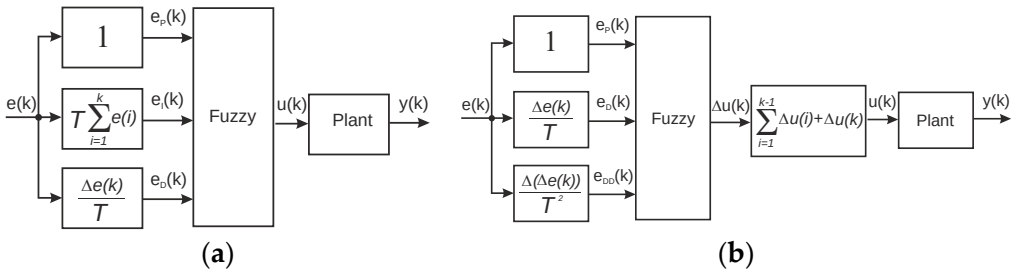

Figure 5. Two versions of the implementation PID fuzzy logic controller: direct (**a**) and incremental (**b**) [16].

The difference between direct and incremental versions is that in the direct controller the control signal $u(k)$ is calculated at any time, and in the incremental controller the control

signal change value $\Delta u(k)$ is calculated. To obtain the value of the control variable $u(k)$ the adder is required; thus, the incremental controller is susceptible to the measure noise. Due to this fact, a direct fuzzy logic controller will be further used.

Figure 6 in a simplified way presents the five stages of fuzzy logic inference, that is: fuzzification, determination of rule firing levels, launching of rules, aggregation of individual rule outputs, and defuzzification. Three tracks (e_P, e_I, e_D) and seven fuzzy sets (NB, NM, NS, Z, PS, PM, and PB) were used to carry out fuzzification. The combination of them gives 147 rules. The Mamdani implication was used to launch rules, then the launched rules were aggregated by the MAX T-conormy operator, and the Center of Gravity method was utilized for defuzzification.

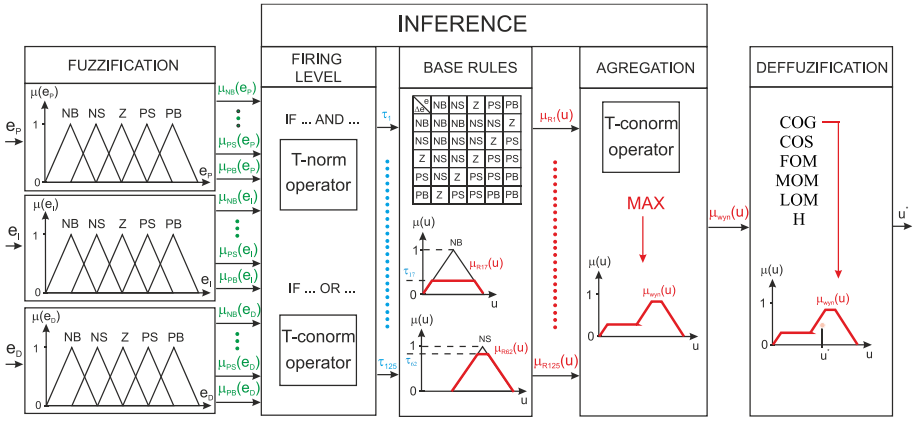

Figure 6. Fuzzy structure [16].

The main problems when designing fuzzy logic controllers concerns the determination of the proper parameters and the structure of the controller. Additionally, the proper membership function must be determined. There are helpful recommendations in the process of designing the controllers that can be found in [21].

The great advantage of fuzzy logic algorithms is their similarity to human control mechanisms. In fact, the algorithm does not need mathematical models describing the behavior of the controlled object [20], but rather human experience and reasoning. There is also the possibility of using the observations of the phase surfaces of conventional controllers, from which fuzzy logic control rules can be derived.

A convenient tool to create the rule base with is the utilization of the template rule base proposed by Mac Vicar-Whelan (Table 1).

Table 1. Mac Vicar-Whelan rule base [16].

Δe\e	NB	NM	NS	Z	PS	PM	PB
NB	NB	NB	NB	NB	NM	NS	Z
NM	NB	NB	NM	NM	NS	Z	PS
NS	NB	NM	NS	NS	Z	PS	PM
Z	NB	NM	NS	Z	PS	PM	PB
PS	NM	NS	Z	PS	PS	PM	PB
PM	NS	Z	PS	PM	PM	PB	PB
PB	Z	PS	PM	PB	PB	PB	PB

The full characteristics of pneumatic elements are required for the proper design of the control system. Especially important are the characteristics of the control valve which can facilitate the designing of the fuzzy logic controller. In the case of the described manipulator, an electro-pneumatic servo-drive is applied. In such a case, fuzzy logic brings extra advantages, as it can eliminate nonlinear aspects of the control process.

Simulation studies were carried out in Matlab/Simulink software using the Fuzzy Logic Toolbox and SimMechanics. A block diagram of the simulation model is shown in Figure 7.

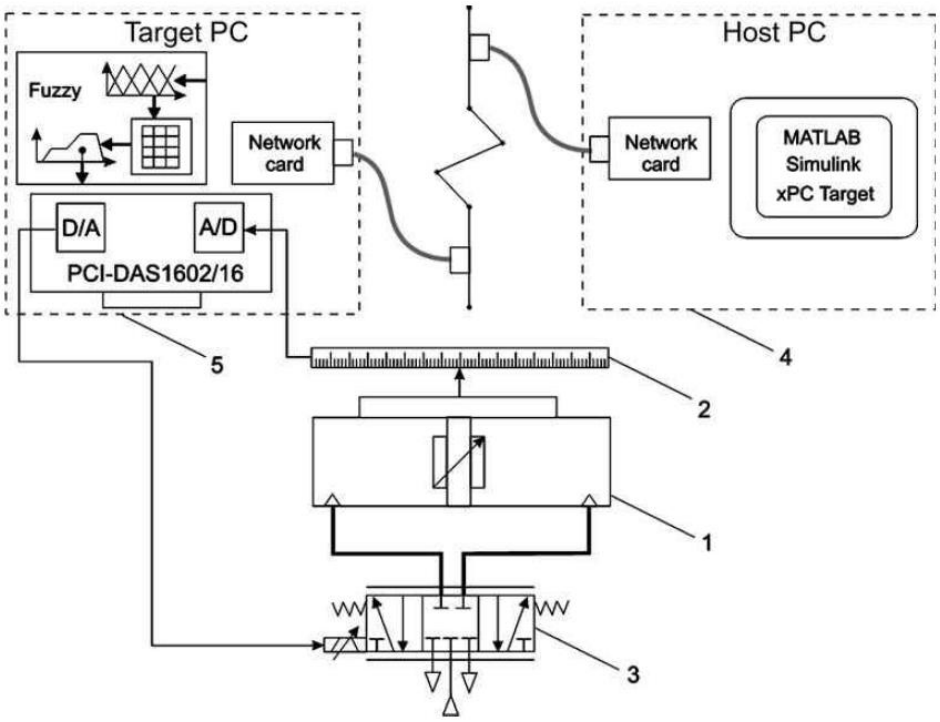

Figure 7. Flow chart of the simulation model: 1—rodless cylinder, 2—position transducer, 3—proportional control valve, 4—computer Host, 5—computer Target.

A simulation study of the positioning of the parallel end-effector of a pneumatically driven planar manipulator was carried out for three motion trajectories. In each case, the manipulator end-effector starts movement from the starting point with coordinates (172,295.6), and then moves to the point with coordinates (300,450). Reference signals, actual signals, and errors are marked on all graphs. Figure 8a shows the trajectory of the end-effector from the start position with coordinates (172,295.6) to the position with coordinates (300,450). Due to the kinematic structure of the manipulator, the derivation of such a trajectory requires the displacement of the manipulator's pneumatic actuators as shown in Figure 8b. Figure 8c on the other hand, shows the x- and y-coordinates of the manipulator end-effector as a function of time.

Subsequent simulations involved the movement of the manipulator end-effector along a square-shaped trajectory (Figure 9a) with a side of 200 mm centered at coordinates (200,500). Introducing such a trajectory required the displacement of the manipulator's pneumatic actuators as shown in Figure 9b,c shows the x and y coordinates of the manipulator end-effector as a function of time.

Figure 10a shows the movement of the manipulator end-effector along a circular trajectory with a radius of 100 mm centered at coordinates (200,450). Introducing such a trajectory required the displacement of the manipulator's pneumatic actuators along sinusoidal trajectories, as shown in Figure 10b. Figure 10c shows the x and y coordinates of the manipulator end-effector as a function of time.

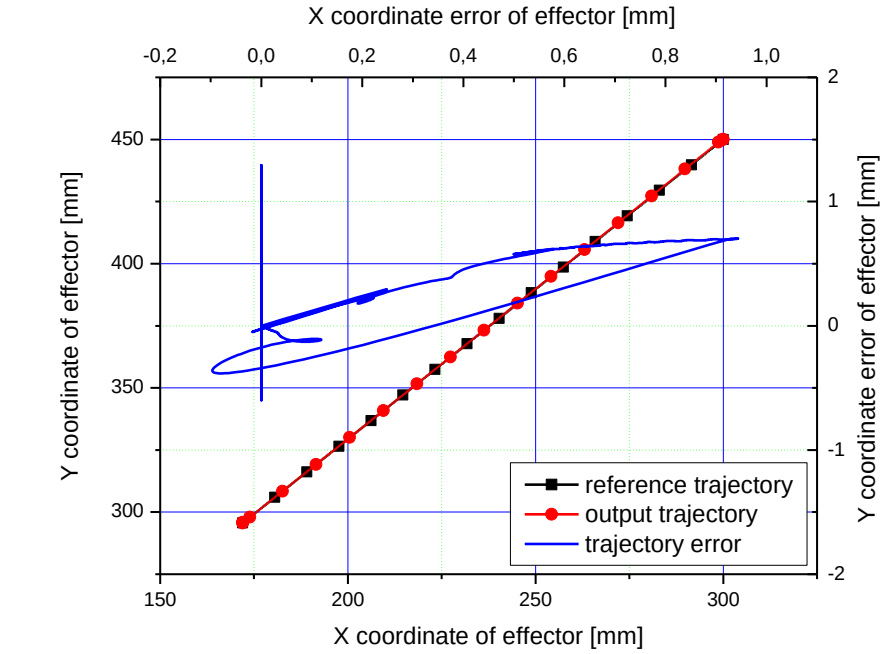

(**a**)

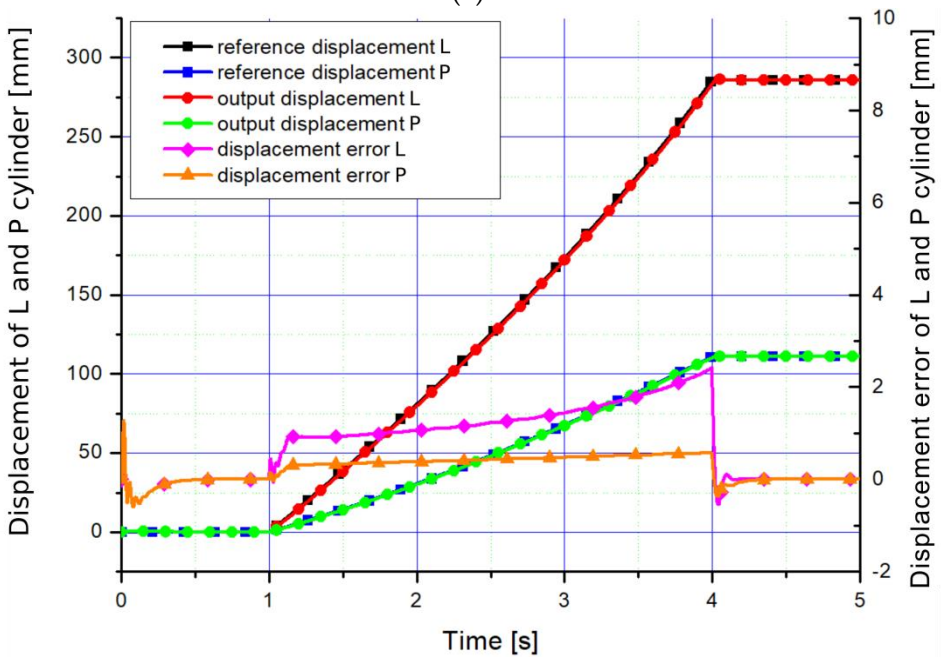

(**b**)

Figure 8. *Cont.*

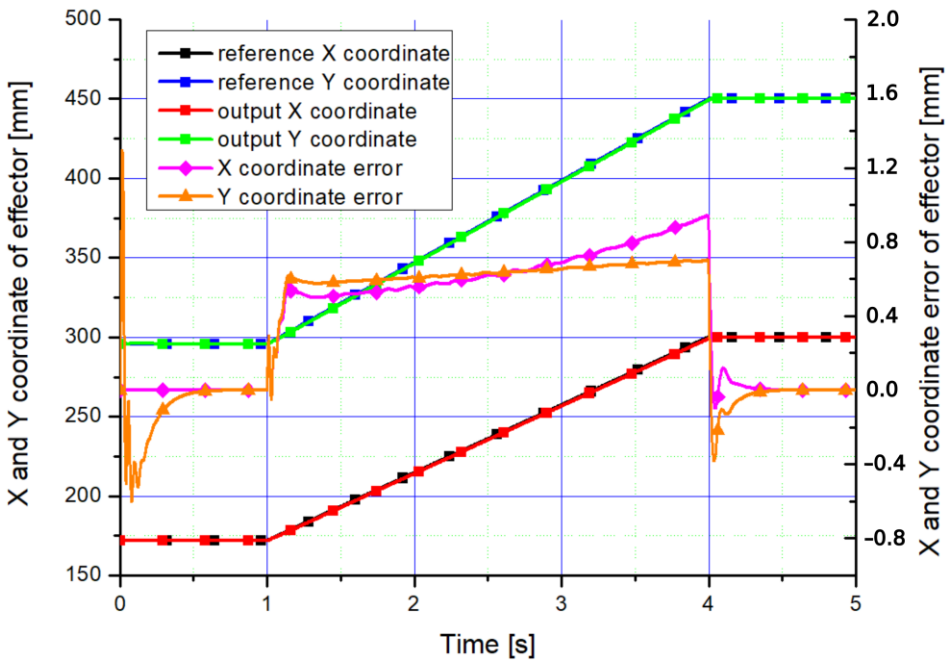

(**c**)

Figure 8. Positioning of the manipulator end-effector from the point (172,295.6) to the point (300,450): (**a**) end-effector trajectory, (**b**) displacement of actuators L and P, (**c**) x- and y-coordinates of the end-effector.

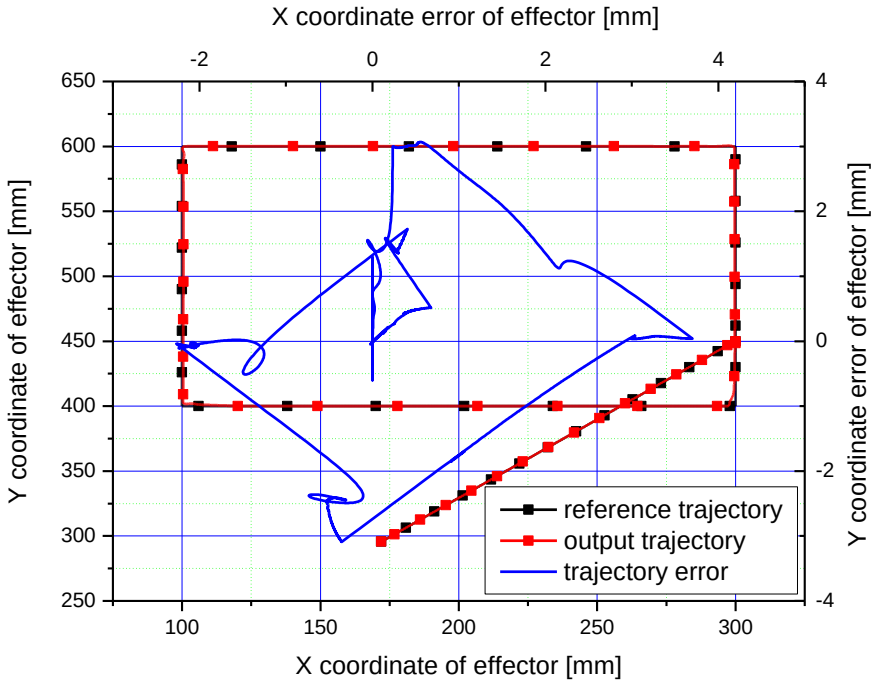

(**a**)

Figure 9. *Cont.*

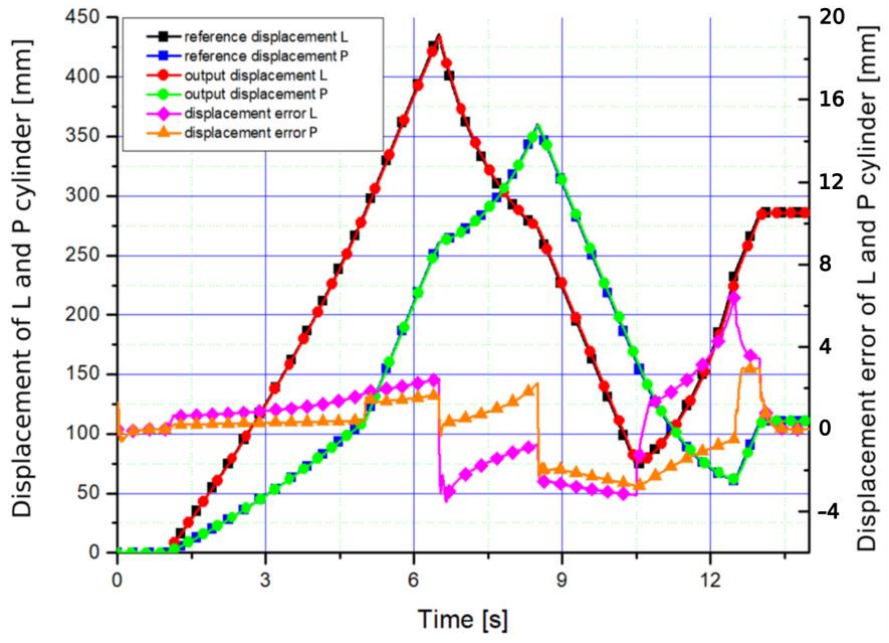

(**b**)

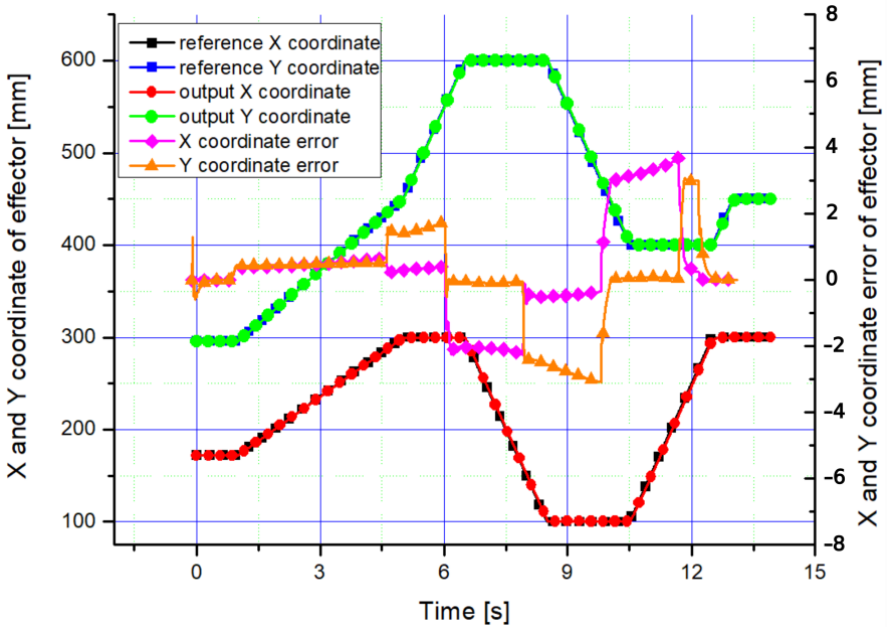

(**c**)

Figure 9. Positioning of the manipulator end-effector along a square trajectory: (**a**) end-effector trajectory, (**b**) displacement of actuators L and P, (**c**) x- and y-coordinates of the end-effector.

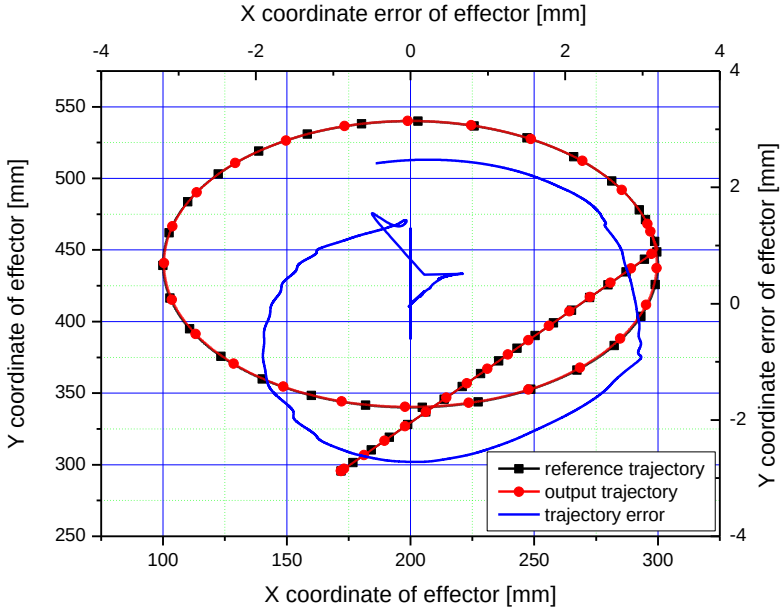

(**a**)

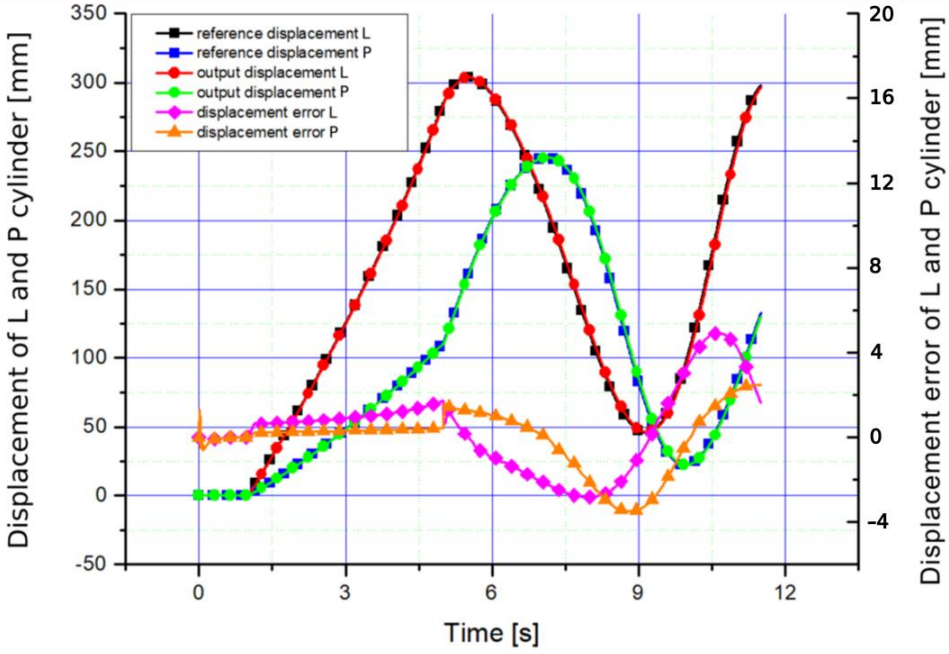

(**b**)

Figure 10. *Cont*.

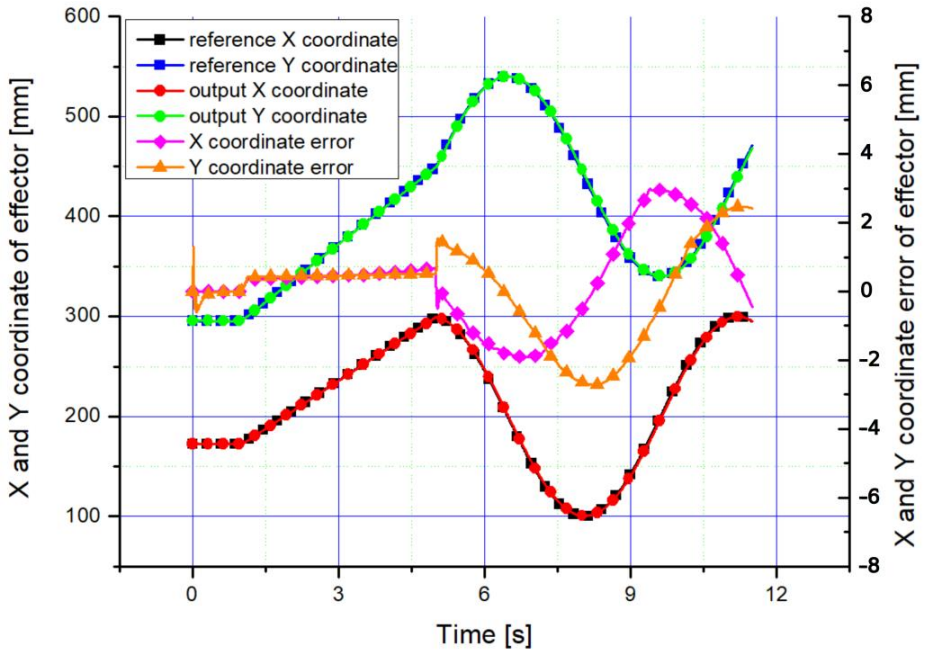

(**c**)

Figure 10. Positioning of the manipulator end-effector along a circular trajectory: (**a**) end-effector trajectory, (**b**) displacement of actuators L and P, (**c**) x- and y-coordinates of the end-effector.

8. Summary and Final Conclusions

This paper focuses on the issues of kinematics, dynamics, and positional control using a fuzzy logic controller. Solid models were presented showing the structure and principle of operation of a pneumatic planar manipulator with a closed kinematic chain. The solid model of the planar manipulator was designed using SolidWorks software. The solid design made it possible to detect collisions and weak points in the designed structure. The preparation of a correct design tested in laboratory conditions is particularly important because it allows the prototype to be made avoiding additional costs associated with design modifications, saves time, and increases the effectiveness of scientific research.

The problem of simple kinematics was determined and solved. Simulation studies were carried out in Matlab/Simulink software using the developed kinematic models of the manipulator, the dynamic models of the electro-pneumatic servo-drive, and studies with positional control using a fuzzy logic controller. The planar manipulator was subjected to simulation studies of the positioning of the end-effector, where it was commanded to:

- Move along a linear trajectory;
- Move along a square trajectory;
- Move along a circular trajectory.

For each manipulator end-effector trajectory, the end-effector coordinates and the displacement of the servo-pneumatic axis actuators were read. The reference values were compared with the actual values, and the control errors were determined.

The simulation results presented confirm the design assumptions made that the proposed model of the planar parallel manipulator and its control system are correct. The reference signals correspond with high accuracy to the obtained signals of the simulation model, which can be observed in the characteristics of the end-effector trajectories by analyzing the deviations for each of the three motion trajectories.

Our further work focuses on experimental investigations of a prototype manipulator on selected trajectories. Prototype tests will be carried out for transposition and follow-up control. Based on the results, we will present a control quality analysis.

Author Contributions: J.T.: Conceptualization, Methodology, Supervision, Project administration, Validation, Writing—review and editing; U.J.-G.: Writing—original draft, Data curation, Visualization, Validation; J.G.: Software, Visualization, Writing—review and editing. All authors have read and agreed to the published version of the manuscript.

Funding: This research received no external funding.

Conflicts of Interest: The authors declare no conflict of interest.

References

1. Zeus, D. Viscous Friction in Small Gaps—Calculations for Non-Contacting Liquid or Gas Lubricated End Face Seals. *Tribol. Trans.* **1990**, *33*, 454–462. [CrossRef]
2. Takosoglu, J.E.; Laski, P.A.; Blasiak, S. A fuzzy logic controller for the positioning control of an electro-pneumatic servo-drive. *Proc. Inst. Mech. Eng. Part I J. Syst. Control Eng.* **2012**, *226*, 1335–1343. [CrossRef]
3. Laski, P.A.; Takosoglu, J.E.; Blasiak, S. Design of a 3-DOF tripod electro-pneumatic parallel manipulator. *Rob. Auton. Syst.* **2015**, *72*, 59–70. [CrossRef]
4. Laski, P.; Blasiak, S.; Takosoglu, J. An Application of a Pneumatic Muscles Actuator for a Delta Pneumatic Manipulator. *Trans. VŠB-Tech. Univ. Ostrava, Mech. Ser.* **2014**, *60*, 43–50. [CrossRef]
5. Šitum, Ž.; Pavkovic, D.; Novakovic, B. Servo Pneumatic Position Control Using Fuzzy PID Gain Scheduling. *J. Dyn. Syst. Meas. Control* **2004**, *126*, 376–387. [CrossRef]
6. Takosoglu, J.; Dindorf, R.; Laski, P. Fuzzy Logic Positioning System of Electro-Pneumatic Servo-Drive. In *Robot Manipulators Trends and Development*; IntechOpen: London, UK, 2010; ISBN 978-953-307-073-5.
7. Kang, B.; Chu, J.; Mills, J.K. Design of high speed planar parallel manipulator and multiple simultaneous specification control. In Proceedings of the 2001 ICRA. IEEE International Conference on Robotics and Automation (Cat. No.01CH37164), Seoul, Korea, 21–26 May 2001; Volume 3, pp. 2723–2728.
8. Kang, B.; Mills, J.K. Dynamic modeling and vibration control of high speed planar parallel manipulator. In Proceedings of the Proceedings 2001 IEEE/RSJ International Conference on Intelligent Robots and Systems. Expanding the Societal Role of Robotics in the the Next Millennium (Cat. No.01CH37180), Maui, HI, USA, 29 October–3 November 2001; Volume 3, pp. 1287–1292.
9. Merlet, J.-P. On the Separability of the Solutions of the Direct Kinematics of a Special Class of Planar 3-RPR Parallel Manipulator. In Proceedings of the International Design Engineering Technical Conferences and Computers and Information in Engineering Conference, Baltimore, Maryland, 10–13 September 2000; pp. 457–462. [CrossRef]
10. Tsai, L.-W. *Robot Analysis: The Mechanics of Serial and Parallel Manipulators*; John Wiley & Sons: Hoboken, NJ, USA, 1999; ISBN 0471325937.
11. Wu, J.; Wang, L.; You, Z. A new method for optimum design of parallel manipulator based on kinematics and dynamics. *Nonlinear Dyn.* **2010**, *61*, 717–727. [CrossRef]
12. Zhang, C.-D.; Song, S.-M. An efficient method for inverse dynamics of manipulators based on the virtual work principle. *J. Robot. Syst.* **1993**, *10*, 605–627. [CrossRef]
13. Denavit, J.; Hartenberg, R.S. A Kinematic Notation for Lower-Pair Mechanisms Based on Matrices. *J. Appl. Mech.* **1955**, *22*, 215–221. [CrossRef]
14. Müller, A. Dynamics of parallel manipulators with hybrid complex limbs—Modular modeling and parallel computing. *Mech. Mach. Theory* **2022**, *167*, 104549. [CrossRef]
15. Chen, Q.; Yang, C. Hybrid algorithm for multi-objective optimization design of parallel manipulators. *Appl. Math. Model.* **2021**, *98*, 245–265. [CrossRef]
16. Takosoglu, J.; Dindorf, R. Wos Piotr Design Rules for Fuzzy Logic Controllers for Pneumatic Systems. In *Advances in Hydraulic and Pneumatic Drives and Control 2020*; Jarosław Stryczek, U.W., Ed.; Springer: Cham, Switzerland, 2021; pp. 192–204, ISBN 978-3-030-59509-8.
17. Putra, M.I.; Irawan, A.; Taufika, R.M. Fuzzy Self-Adaptive Sliding Mode Control for Pneumatic Cylinder Rod-Piston Motion Precision Control. *J. Phys. Conf. Ser.* **2020**, *1532*, 12028. [CrossRef]
18. Baba, A.F.; Safak, C.; Topuz, V. *Genetic-Fuzzy Controller Design for Pneumatic Motors: Speed Control*; LAP LAMBERT Academic Publishing: Sunnyvale, CA, USA, 2011; ISBN 3-8443-9833-3.
19. Takosoglu, J.E. Control System of Delta Manipulator with Pneumatic Artificial Muscles. In Proceedings of the Engineering 22nd International Conference, Engineering Mechanics, Svratka, Czech Republic, 9–12 May 2016; pp. 546–549.
20. Yager, R.; Filev, D. *Essentials of Fuzzy Modeling and Control*, 1st ed.; John Wiley & Sons: Hoboken, NJ, USA, 1994.
21. Driankov, D.; Hellendoorn, H. *Reinfrank. Michael, An Introduction to Fuzzy Control*, 2nd ed.; Springer: Berlin/Heidelberg, Germany, 1996; ISBN 978-3-642-08234-4.